

## Surface Interactions and Fouling Properties of *Micrococcus luteus* with Microfiltration Membranes

Lei Feng · Xiufen Li · Ping Song · Guocheng Du · Jian Chen

Received: 17 November 2010 / Accepted: 10 August 2011 /  
Published online: 26 August 2011  
© Springer Science+Business Media, LLC 2011

**Abstract** This study was conducted to investigate microbial adhesion of *Micrococcus luteus* to polypropylene (PP) and polyvinylidene fluoride (PVDF) membranes in relation to the variation of the interfacial energies in the membrane–bacteria systems, for revealing effects of short-range surface interactions on filtration behavior. Both the membranes and *M. luteus* showed typical strong electron donors and hydrophilic properties. The AB component was dominant in the interfacial energies of the two membrane–bacteria systems. *M. luteus* presented larger negative  $U_{\text{mlb}}^{\text{XDLVO}}$  to the PP membrane than to the PVDF membrane. The adhesion experiments also proved that *M. luteus* had higher adhesion percentage to the PP membrane. This study demonstrated that the adhesion potentials of *M.*

---

L. Feng  
Resource and Environment College, Fujian Agriculture and Forestry University,  
Fuzhou 350002 Fujian province, People's Republic of China  
e-mail: fengleisp@126.com

L. Feng · X. Li (✉)  
Laboratory of Environmental Biotechnology, School of Environment and Civil Engineering,  
Jiangnan University, Wuxi 214122 Jiangsu province, People's Republic of China  
e-mail: xfli@jiangnan.edu.cn

P. Song  
College of Forestry, Fujian Agriculture and Forestry University, Fuzhou 350002 Fujian province,  
People's Republic of China

G. Du  
School of Biotechnology, Jiangnan University, Wuxi 214122 Jiangsu province,  
People's Republic of China

J. Chen (✉)  
National Key Lab. of Food Science and Technology, Jiangnan University,  
Wuxi 214122 Jiangsu province, People's Republic of China  
e-mail: jchen@jiangnan.edu.cn

*luteus* to the PP and PVDF membranes might be explained in terms of bacterium, membrane, and intervening medium surface properties, which are mainly determined by the interfacial energies in the systems according to the XDLVO theory.

**Keywords** *Micrococcus luteus* · Biofouling microfiltration · Interfacial energy · The XDLVO theory

## Introduction

In recent years, the application of membrane bioreactor (MBR) in wastewater treatment and reclamation received considerable attention, since they exhibit many advantages relating to product quality and required footprint compared to conventional process. In spite of many merits of the membrane technology, however, its vast and successful application for wastewater purification is greatly limited by membrane biofouling, which causes severe performance loss, requiring costly periodic cleaning or membrane replacement and so increasing operating costs and/or decreasing plant output [1, 2].

The nature of membrane biofouling is a consequence of mature biofilm formation in the pores or on the surface of the membrane [3, 4], in which bacterial adhesion is considered the first stage and acts a critical role. As a prerequisite of the formation of biofilms on substratum surfaces, the mechanisms involved in bacterial adhesion are complex and generally governed by the extended DLVO (XDLVO) theory through calculating the interaction energy as a function of separation distance [5]. According to the XDLVO viewpoint, bacterial adhesion and surface colonization are correlated with the interfacial energy components in terms of Lifshitz–van der Waals interactions, acid–base interactions, and electrostatic interactions, which are mainly determined by the physicochemical properties of bacterial cell and substratum surfaces, as well as the intervening medium [6].

A number of previous studies have successfully described the microorganism adhesion properties for various substrata related to the variation of interfacial energies. For example, Li et al. [7] investigated the adhesion properties of eight different bacteria to the glass and metal-oxide surfaces. It was noted that bacterial adhesion ability might be increased by the presence of the type of metal oxide and was significantly correlated with total adhesion free energy between the bacteria and the surface. Lopes et al. [8] reported that *Desulfovibrio desulfuricans* strain showed a higher adhesion number to the metallic nickel than the stainless steel and polymethylmethacrylate, and the reason of the higher number could be explained by differences in hydrophobicity, in roughness and in the electron-acceptor character of the substrata. With respect to membrane filtration systems, only Brant et al. [9] assessed the short-range surface interactions of membrane process. However, their investigation objects were several RO membranes and abiotic colloids. There was little information on interfacial energy properties related to the permeation behaviors of MF membrane–bacteria systems, particularly concerning the preponderant bacteria in the biofouling layer of MBR.

In this work, *Micrococcus luteus*, a dominant strain extracted from the membrane biofouling layer of MBR, was firstly isolated and tested as a model microorganism. Then, the surface physicochemical properties and the static adsorption of the strain to the membrane surface were investigated. The aim of this work was to provide some available and valuable information on the evaluation of membrane biofouling mechanisms in the MBR wastewater treatment.

## Interfacial Interaction Profiles

### Surface Tension

The surface tensions of each membrane and the bacterial cell were calculated according to Van Oss–Chaudhury–Good equation [7, 10]:

$$r^{\text{TOT}} = r^{\text{LW}} + r^{\text{AB}} \quad (1)$$

$$r^{\text{AB}} = 2\sqrt{r^+ r^-} \quad (2)$$

$$(1 + \cos \theta) r_1^{\text{TOT}} = 2 \left( \sqrt{r_s^{\text{LW}} r_l^{\text{LW}}} + \sqrt{r_s^+ r_l^-} + \sqrt{r_s^- r_l^+} \right) \quad (3)$$

Where  $\theta$  is the contact angle,  $r^{\text{TOT}}$  the total surface tension,  $r^{\text{LW}}$  the LW component of surface tension,  $r^{\text{AB}}$  the AB component of surface tension, and  $r^+$  and  $r^-$  are electron-acceptor and electron-donor parameters of the polar component of the surface tension, respectively. The subscript (s) denotes solid surface (membrane or cell), and (l) refers to the liquid used in each measurement.

### Free Energy of Interaction

The free energy of interaction caused by Lifshitz–Van der Waals ( $\Delta G^{\text{LW}}$ ) and acid–base interactions ( $\Delta G^{\text{AB}}$ ) between the *M. luteus* cells and the membranes immersed in water was given by [10, 11]:

$$\Delta G^{\text{LW}} = 2 \left( \sqrt{r_l^{\text{LW}}} - \sqrt{r_m^{\text{LW}}} \right) \left( \sqrt{r_b^{\text{LW}}} - \sqrt{r_l^{\text{LW}}} \right) \quad (4)$$

$$\Delta G^{\text{AB}} = 2\sqrt{r_l^+} \left( \sqrt{r_m^-} + \sqrt{r_b^-} - \sqrt{r_l^-} \right) + 2\sqrt{r_l^-} \left( \sqrt{r_m^+} + \sqrt{r_b^+} - \sqrt{r_l^+} \right) - 2 \left( \sqrt{r_m^+ r_b^-} + \sqrt{r_b^+ r_m^-} \right) \quad (5)$$

The subscripts m, b, and l denote the membranes (polyvinylidene fluoride, PVDF, or polypropylene, PP), *M. luteus* cell, and water, respectively.

### Interfacial Energy Calculations

In this study, the bacterial cells and the membranes were considered as perfectly smooth spheres and flat planes, respectively. According to the XDLVO theory [6], the total interfacial energy ( $U_{\text{mlb}}^{\text{XDLVO}}$ ) needed to bring a bacterium (b) from an infinite distance to a membrane surface (m) in water (l) was calculated by:

$$U_{\text{mlb}}^{\text{XDLVO}} = U_{\text{mlb}}^{\text{LW}} + U_{\text{mlb}}^{\text{EL}} + U_{\text{mlb}}^{\text{AB}} \quad (6)$$

Where  $U_{\text{mlb}}^{\text{LW}}$ ,  $U_{\text{mlb}}^{\text{EL}}$ , and  $U_{\text{mlb}}^{\text{AB}}$  are the individual components of the total interfacial energy arising from LW, EL, and AB forces, respectively. The individual components may be written as [7, 9]:

$$U_{\text{mlb}}^{\text{LW}} = 2\pi\Delta G_{h_0}^{\text{LW}} \frac{h_0^2 a}{h} \quad (7)$$

$$U_{\text{mlb}}^{\text{AB}} = 2\pi a \lambda \Delta G_{h_0}^{\text{AB}} \exp \left[ \frac{h_0 - h}{h} \right] \quad (8)$$

$$U_{\text{mlb}}^{\text{EL}} = \pi \varepsilon a \left[ 2\zeta_b \zeta_m \ln \left( \frac{1 + e^{-kh}}{1 - e^{-kh}} \right) + (\zeta_b^2 + \zeta_m^2) \ln(1 - e^{-2kh}) \right] \quad (9)$$

Where  $a$  is the radius of the *M. luteus* cell, and  $h_0$  is the minimum separation distance between the bacterium and the membrane, which is usually defined as 0.158 nm [12].  $h$  is the surface to surface separation distance between the membrane and the *M. luteus* cell.  $\lambda$  is the decay length of AB interactions, whose value is 0.6 nm in aqueous systems [10].  $\varepsilon$  is the dielectric permittivity of the suspending fluid,  $k$  the inverse Debye screening length, and  $\zeta_m$  and  $\zeta_b$  are the surface potentials of the membrane and *M. luteus* cell, respectively.

## Experimental Protocols

### Model Microorganism

*M. luteus*, which was also a common microorganism presented in activated sludge [13, 14], was isolated as the dominant strain from a biofouled microfiltration membrane in a pilot submerged MBR. The operating conditions and synthetic wastewater components of the MBR described in the previous work [15] were shown in Table 1 and 2, respectively.

The strain was cultivated in shake flasks at 30 °C with shaking at 200 rpm. A defined liquid medium (DLM) which had the same composition as the synthetic wastewater in the MBR was used for the cultivation. The bacterial cells at the late logarithmic growth phase were collected by centrifuging at 5,000×g for 15 min.

### Representative Membranes

Disk-shaped PVDF and PP plate membranes were adopted in this study, which were purchased from Shanghai Jingxi chemistry engineering Co. Ltd. Both the membrane

**Table 1** Stable operation conditions of MBR

Parameters	Values	Parameters	Values
DO (mg L <sup>-1</sup> )	4.0±0.5	Temperature (°C)	25±1
pH	7.0±0.2	Influent COD (mg L <sup>-1</sup> )	600±20
Flux (L m <sup>-2</sup> h <sup>-1</sup> )	5.0±0.2	Effluent COD (mg L <sup>-1</sup> )	35±5
Hydraulic retention time (HRT) (h)	8.0±0.3	Influent NH <sub>4</sub> -N (mg L <sup>-1</sup> )	25±2
Sludge retention time (SRT) (days)	No discharge	Effluent NH <sub>4</sub> -N (mg L <sup>-1</sup> )	1.0±0.2
Mixed liquor suspended solids (MLSS) (g L <sup>-1</sup> )	10±1		

**Table 2** Components and quality of synthetic wastewater (milligrams per liter)

Components	Concentration (mg L <sup>-1</sup> )	Components	Concentration (mg L <sup>-1</sup> )
Industrial glucose	600±10	CaCl <sub>2</sub>	10±2
Yeast extract	30±4	MnCl <sub>2</sub>	2±0.5
Peptone	20±4	FeSO <sub>4</sub>	0.3±0.1
MgSO <sub>4</sub> ·7H <sub>2</sub> O	10±2	KH <sub>2</sub> PO <sub>4</sub>	20±3
NH <sub>4</sub> Cl	80±5		

disks, with diameter 80 mm, had a nominal pore size of 0.22 µm and a thickness of 145 µm. The experiments were conducted using a Plexiglas dead-end filtration module (Shanghai Institute of Applied Physics, China), which had a valid volume of 500 mL and 60 mm inner diameter, corresponding to an effective membrane area of 28.26 cm<sup>2</sup>.

### Contact Angle Measurements

Contact angle measurements of the surfaces of the membranes and the bacterium were performed in triplicate using a goniometer with the aid of an image analysis system (DSA100, Kruss Instruments Corp., Germany) by the sessile drop method [7, 9].

### Surface Charge Measurements

Zeta potential of the bacterium was calculated from electrophoretic mobility. The cells prepared as described above were re-suspended in a 1-mM KCl solution, and the zeta potential was measured five times using a Zetasizer analyzer (Nano-ZS90, Malvern Instruments Corp., UK). Zeta potentials of the membranes were determined using a streaming potential analyzer (BI-EKA, Brookhaven Instruments Corp., USA) [16, 17].

### Adsorption Assays

The *M. luteus* cell was suspended in 1 mM sterilized KCl solution at a concentration of  $2 \times 10^8$  cells/mL ( $OD_{600}=0.59$  in 1.5-cm-diameter tubes). Then the adsorption assay experiments were conducted using the Plexiglas dead-end filtration module (described in the [Representative membranes](#) section). For each type of membrane, four identical membrane filtration modules were applied. Three-hundred milliliters of bacterial suspension was charged into each membrane filtration module without applying pressure but stirring gently. Every 20-min interval, one filtration module was dismantled, and the membrane was gently rinsed with filtered–sterilized distilled water in order to remove poorly adhered bacteria. The cells were separated from the membranes by sonicating at 10% power for 30 s with an ultrasonic processor (XLNS-1001, Changzou New Concept Instruments Corp., China). The preliminary experiment suggested that this sonicating conduct could effectively remove the adhered bacteria of both membranes and had an insignificant cell lysis. The separated cell suspension was diluted and inoculated onto 20% DLM agar plates and incubated at 30 °C for 72 h. The numbers of CFU of *M. luteus* adsorbing on different membranes were then calculated.

## Results and Discussion

### Surface Thermodynamic Properties of Bacterial Cell and Membrane

Surface thermodynamic properties of *M. luteus* cell and the two types of membranes were calculated through the measurement of the contact angles with water, glycerol, and diiodomethane (Table 3). Higher values of  $r^-$  than those of  $r^+$  were found for both the membranes and the strain. It is particularly true for *M. luteus* and the PVDF membrane, of which the  $r^-$  values were two orders of magnitude greater than the  $r^+$  values, exhibiting the trait of a typical high electron donor. This result was consistent with previous studies [9, 18, 19] where polymeric membranes and bacterial strains were typically characterized by a high electron donor monopolarity. The *M. luteus* strain displayed an  $r^{LW}$  value of 47.31 mJ/m<sup>2</sup>, which was a typical value for bacterial strains [20]. Compared with the PP membrane, *M. luteus* and the PVDF membrane had higher values of  $r^{TOT}$  owing to their relatively larger  $r^{LW}$  and  $r^{AB}$  values. Additionally, the surfaces of the two membranes and the bacterium were negatively charged with the various zeta potentials under the investigated conditions, indicating an asymmetric feature involved in EL double layer interactions between the membranes and the bacterium surfaces. Furthermore, the free energy of cohesion ( $G_{sws}$ ), representing the interaction free energy when two surfaces of the same material (membrane or bacterium) were immersed in a solvent (water) [9, 10], was calculated in Table 2. The result showed that both the bacterium and the membranes were hydrophobic based on their negative values of  $G_{sws}$ . However, the PP membrane showed a relatively stronger hydrophobicity than others.

### Interfacial Energy Analysis

Figure 1 showed the profiles of the various interfacial energy components vs. separation distance for the two membrane–bacterium systems. According to the XDLVO theory, when the total interfacial energy of the membrane–bacterium system is negative, the bacterial adsorption to filtration membrane can occur. In this work, highly attractive properties of the AB and LW interaction components in both the membrane–bacteria combinations were expected from the negative values in a short range ( $h < 5$  nm). On the contrary, the *M. luteus* cell's getting close to membranes was subjected to the repulsive EL interaction because the

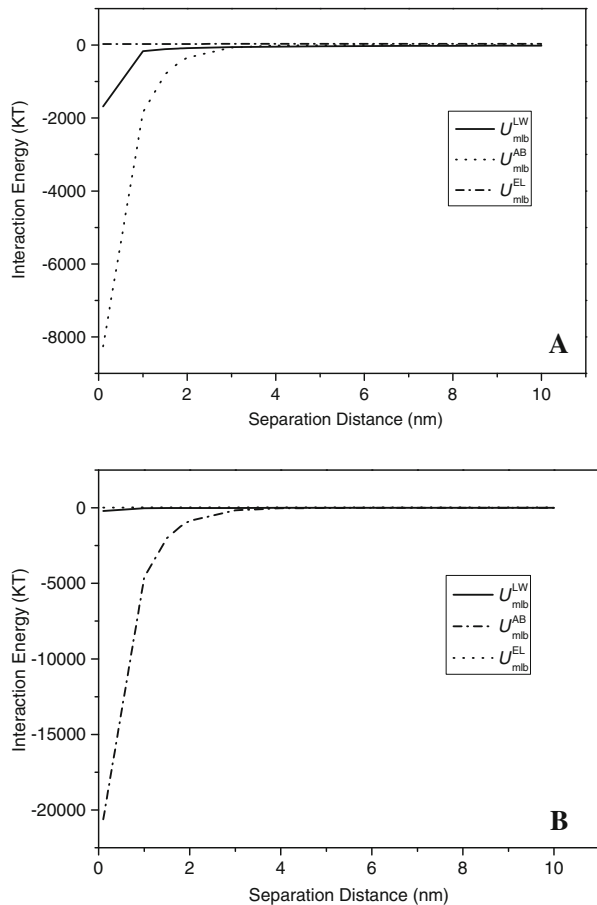
**Table 3** Surface thermodynamic properties of bacteria and membrane

Surface	$\theta^{\text{Dii}}$ (°)	$\theta^{\text{GL}}$ (°)	$\theta^{\text{W}}$ (°)	$\gamma^{\text{LW}}$ (mJ/m <sup>2</sup> )	$\gamma^-$ (mJ/m <sup>2</sup> )	$\gamma^+$ (mJ/m <sup>2</sup> )
<i>M. luteus</i>	21.25±1.69	42.06±1.74	51.91±2.11	47.31	19.07	0.86
PVDF	34.84±1.58	50.53±2.31	59.88±1.27	42.10	15.49	0.79
PP	67.96±2.85	86.97±1.67	98.13±2.33	24.02	1.74	0.11

Surface	$\gamma^{\text{AB}}$ (mJ/m <sup>2</sup> )	$\gamma^{\text{TOT}}$ (mJ/m <sup>2</sup> )	$G_{\text{sWS}}$ (mJ/m <sup>2</sup> )	Zeta potential (mv)	Radius (μm)
<i>M. luteus</i>	8.11	55.42	−21.02	−18.60±2.43	0.55±0.07
PVDF	7.0	49.10	−25.15	−22.10±3.32	
PP	0.87	24.89	−70.39	−15.80±2.41	

$\theta^{Dii}$  diiodomethane contact angle,  $\theta^{GL}$  glycerol contact angle,  $\theta^W$  water contact angle,  $\theta_{sws}$  the free energy of interaction between two surfaces of the same material immersed in water

**Fig. 1** Interaction energy component variation of bacterial adsorption to PVDF membrane (a) and PP membrane (b) as a function of separation distance



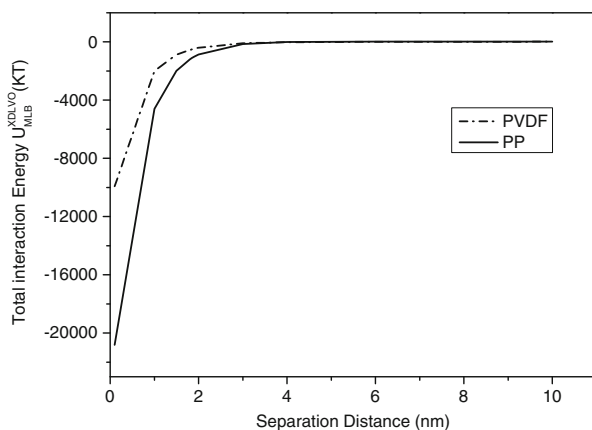
two membranes and the bacterium were all negatively charged. Among the various interfacial surface energy components, the AB interactions of both membrane–bacterium combinations had the smallest (negatively greatest) values at the specific separate distance ( $h < 5$  nm), which was mainly attributed to the hydrophobic nature of the membrane and bacterium surfaces. This suggested that the Lewis acid–base interaction was the dominant driving force on *M. luteus* strain adhesion to the two tested membranes.

The total interfacial surface energy ( $U_{mwb}^{XDLVO}$ ) curves of both membrane–bacterium systems were presented in Fig. 2. *M. luteus* strain showed negative  $U_{mwb}^{XDLVO}$  values to the PP and PVDF membranes, demonstrating the adhesion potentials to these substrates. When compared with the *M. luteus*–PVDF membrane combination, the *M. luteus*–PP membrane combination had a lower (negatively greater)  $U_{mwb}^{XDLVO}$  value. Depending on this result, theoretically, *M. luteus* strain might be favored to the PP membrane than to the PVDF membrane.

#### Bacterial Adhesion and Fouling Analysis

Figure 3 presented the results of static adsorption tests. It could be seen that the adhesion amounts of *M. luteus* to both the membranes markedly increased with the processing time

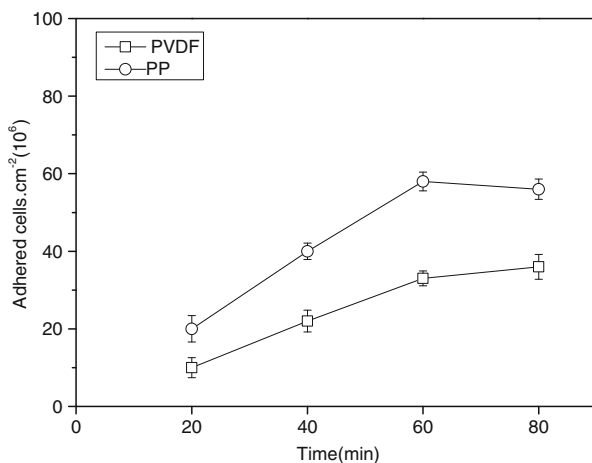
**Fig. 2** Total interaction energy variation of bacterial adsorption to PVDF and PP membranes as a function of separation distance



at initial stage, while after 60 min, they turned out to be steady. It should be emphasized that despite the similar adhesion tendency of *M. luteus* strain to both the membranes, stronger colonizing ability of the strain in the PP membrane was exhibited compared with that in the PVDF membrane. This result agreed well with the above interfacial surface energy prediction based on the XDLVO approach, in which the *M. luteus*–PP system had a larger negative value.

Initial microbial deposition is a critical early stage event in the overall process of biofouling. Several previous studies revealed that primary adhesion of cells—at a particular growth stage and adapted to a fixed nutrient environment—was largely controlled by interfacial forces [7, 9]. The results of our present study also supported this point. However, bacterium filtration involves a complicated process, which can be divided into various individual steps including pore blocking, cake filtration, compressibility, extracellular polymer secretion, etc. [21, 22]. Although our work did not achieve a quantitative explanation for the mechanism of interfacial energy during the entire filtration period, it may be speculated that *M. luteus* strain has a more severe fouling to the PP membrane as the PP membrane can adsorb more bacteria at the beginning of the filtration basing on the XDLVO prediction and the static adhesion result and thus lead to more colonization, EPS

**Fig. 3** Adsorption of *M. luteus* to PVDF and PP membranes





secretion, and greater difficulty in backwashing or scouring bacteria away from the PP membrane surface.

## Conclusion

In the present work, the biofouling of *M. luteus* strain to the PP and the PVDF membranes was investigated regarding the variations of interfacial energies, which were calculated according to independently determined bacterium, membrane, and solution surface thermodynamic properties. It was found that surfaces of both the bacterium and the membranes had the significant electron donor traits, charged by negative potentials. The AB interaction played a crucial role in the interfacial energies of both the membrane–bacteria combinations. The stronger hydrophobic properties of the PP membrane resulted in significantly lower  $U_{mlb}^{AB}$  value (negatively greater) than that of the PVDF membrane. The experiment results of static adhesion indicated that the bacterial deposition to the PP and PVDF membranes was determined to a great extent by the interfacial energies in the membrane–bacteria systems. Such result also suggested that independently measured surface thermodynamic properties could be used to predict the relative propensity of bacterial membrane fouling. Our future work will try to adjust the membrane surface thermodynamic properties by various surface modification technologies, in order to weaken the system interfacial energies and, in turn, the microbial membrane biofouling potential.

**Acknowledgments** This work is supported by a grant from the Major State Basic Research Development Program (973 Program) of China (no. 2007CB714036) and the National Natural Science Foundation of China (no. 50678073).

## References

- Kim, A. S., Chen, H., & Yuan, R. (2006). *Journal of Colloid and Interface Science*, 303, 243–249.
- Lodge, B., Judd, S. J., & Smith, A. J. (2004). *Journal of Membrane Science*, 231, 91–98.
- Zhang, K., Choi, H., Dionysiou, D. D., Sorial, G. A., & Oerther, D. B. (2006). *Environmental Microbiology*, 8, 433–440.
- Badireddy, A. R., Chellam, S., & Yanina, S. (2007). *Biotechnology and Bioengineering*, 99, 634–643.
- Bos, R., Mei, H. C., & Busscher, H. J. (1999). *FEMS Microbiology Reviews*, 23, 179–230.
- Sharma, P. K., & Hanumantha Rao, K. (2003). *Colloids and Surfaces. B, Biointerfaces*, 29, 21–38.
- Li, B., & Logan, B. E. (2004). *Colloids and Surfaces. B, Biointerfaces*, 36, 81–90.
- Lopes, F. A., Morin, P., Oliveira, R., & Melo, L. F. (2005). *Colloids and Surfaces. B, Biointerfaces*, 46, 127–133.
- Brant, J. A., & Childress, A. E. (2002). *Journal of Membrane Science*, 203, 257–273.
- Van Oss, C. J. (1993). *Colloids and Surfaces A: Physicochemical and Engineering Aspects*, 78, 1–49.
- Wu, W., & Nancollas, G. H. (1999). *Colloids and Surfaces. B, Biointerfaces*, 14, 57–66.
- Bhattacharjee, S., Sharma, A., & Bhattacharya, P. K. (1996). *Industrial and Engineering Chemistry Research*, 35, 3108–3121.
- Leung, W.C., Wong, M.F., Chua, H., Lo, W., Yu, P.H.F., and Leung, C.K. (2000). *Water science and technology*, 41, 233–240.
- Wagner, M., Erhart, R., Manz, W., Amann, R., Lemmer, H., Wedi, D., et al. (1994). *Applied and Environmental Microbiology*, 60, 792–800.
- Li, X. F., Li, Y. J., Liu, H., Hua, Z. Z., Du, G. C., & Chen, J. (2008). *Separation and Purification Technology*, 59, 26–33.
- Elimelech, M., Chen, W. H., & Waypa, J. J. (1994). *Desalination*, 95, 269–286.

17. Nyström, M., Lindström, M., & Matthiasson, E. (1989). *Colloids and Surfaces*, 36, 297–312.
18. Bouchard, C. R., Jolicœur, J., Kouadio, P., & Britten, M. (1997). *The Canadian Journal of Chemical Engineering*, 75, 339–345.
19. Gourley, L., Britten, M., Gauthier, S. F., & Pouliot, Y. (1994). *Journal of Membrane Science*, 97, 283–289.
20. Chen, G., & Zhu, H. (2005). *Colloids and Surfaces. B, Biointerfaces*, 44, 41–48.
21. Xu, W., & Chellam, S. (2005). *Environmental Science and Technology*, 39, 6470–6476.
22. Chellam, S., & Xu, W. (2006). *Journal of Colloid and Interface Science*, 301, 248–257.